Acta Crystallographica Section A
Foundations of Crystallography
ISSN 0108-7673

Received 19 January 2007
Accepted 4 May 2007

Topological relations between three-dimensional periodic nets. I. Uninodal nets

Vladislav A. Blatov

Samara State University, Ac. Pavlov St. 1, Samara 443011, Russia. Correspondence e-mail: blatov@ssu.samara.ru

A method is proposed to search for topological relations between periodic nets. The method is based on a sequence of steps of decreasing the node degree and symmetry of the initial net (supernet) and, as a result, gives all its subnets. It is implemented into the program package *TOPOS* which automatically constructs the net relation graph (NRG) for a given set of initial nets. The method is used to find all supernet–subnet relations for 924 initial 4–12-coordinated uninodal nets. The resulting NRG consists of 6528 3–12-coordinated uninodal nets; 5278 of them have topologies not described earlier. It is shown that many NRG properties are useful in crystal chemistry. In particular, a path between NRG nodes corresponds to a sequence of transformations that relate the nets, the adjacency sequence of a NRG node may be used as a criterion for crystallochemical 'significance' of the corresponding net. Many well known net topologies are found to have a large number of relations with other topologies that cause their special place in the NRG and crystallochemical 'significance'. The peculiarities of the proposed approach are illustrated by examples of the nets often occurring in crystal structures.

1. Introduction

The concept of periodic ***nets***[1] plays an important role in modern crystal chemistry. Starting from pioneer works of Wells (1954, 1977), this concept was highly developed in the 1980s–90s (O'Keeffe & Hyde, 1996) and became a powerful tool to analyse the topological properties of crystal structures. Many topological parameters of periodic nets, such as node degree, coordination sequence, ring size, interpenetration pattern, have a chemical meaning and are used in supramolecular chemistry, crystal engineering and design (Öhrström & Larsson, 2005; Koch *et al.*, 2006; Carlucci *et al.*, 2007). In the last decade, other topological constructions based on the periodic nets, namely tilings and dual nets, appeared in the literature (Delgado-Friedrichs *et al.*, 2005; Hyde *et al.*, 2006).

However, until recently, the properties of individual nets were mainly analysed, and much less attention was paid to hierarchical relations between nets and to the methods of their mutual transformations. Although these problems were of great interest in crystal chemistry long ago, the results were usually not systematic and were obtained with time-consuming visual and handmade analysis. The most extensive work (not finished yet) has been that to consider relations between sphere packings (see Koch *et al.*, 2006, and references therein). Some net–***subnet*** relations are gathered in the RCSR[2] database. Knowing the relations between nets, one can find possible ways of transitions from one net to another. All the transition pathways pass through a common subnet of the related nets. The condition of preserving the three-dimensional connected subnet during the transition requires that the subnet space group has to be a common subgroup of the space groups of initial and target nets. This approach was applied to consider in detail possible phase transitions for NaCl–CsCl, ZnS (zinc-blende)–NaCl, ZnS (wurtzite)–NaCl, quartz–tridimite and diamond–lonsdaleite structure-type pairs (Sowa & Koch, 2001, 2002; Sowa, 2005, and references therein). An alternative approach based on periodic surfaces was developed as well (Leoni & Zahn, 2004, and references therein).

The hierarchical net–subnet relations could help to answer the question: why do some nets often occur in nature, whereas other nets have never been found? This question is similar to some extent to the question about frequent and rare space groups in crystals, but requires a topological, not geometrical, approach to be focused on the system of chemical bonds, not on the details of atomic or molecular packings. Thus, Ockwig *et al.* (2005) studied 1127 metal-organic frameworks and found that in 20.7% of them the diamond (**dia**, 4/6/*c*1)[3] topological motif occurred, and other frequent topological types of nets were primitive cubic lattice (**pcu**, 6/4/*c*1, 12.9%) and

[1] The definitions of the basic terms marked as bold italic are given in Appendix *A*. For more complete information on the terminology relating to crystal nets and graphs, see Delgado-Friedrichs & O'Keeffe (2005) and Carlucci *et al.* (2007).

[2] Reticular Chemistry Structure Resource, http://rcsr.anu.edu.au/.

[3] Hereafter, the RCSR three-letter symbols (if any) are used for nets. Fischer's symbols *k*/*m*/*fn* (*cf.* Koch *et al.*, 2006) are given for sphere packings together with the RCSR names.

3-coordinated **srs** (3/10/*c*1, 6.4%) nets. It was found that the nets with high frequency are topologically highly symmetrical and, in particular, have small numbers of kinds of nodes and edges. Thus, ***uninodal*** and ***edge-transitive*** nets must be of special interest in crystal design (Delgado-Friedrichs *et al.*, 2006). Similar results were obtained for interpenetrating metal-organic (Blatov *et al.*, 2004) and inorganic (Baburin *et al.*, 2005) frameworks; albeit the numbers for net frequencies were different, the first triple of nets (**dia**–**pcu**–**srs**) was the same.

One of the main obstacles in understanding net–subnet relations is lack of a general algorithm for enumerating periodic subnets. A strict graph-theoretical approach based on the representation of a net as a ***labelled quotient graph*** (Klein, 1996; Klee, 2004; Eon, 2005) has serious computational difficulties and up to now has not been implemented as an available computer application. Moreover, because the number of periodic subnets for a given periodic net is generally infinite, one needs some restriction criteria to select crystallochemically 'significant' nets. At present, the electronic resources that collect such 'significant' nets are the RCSR database and the TTD[4] collection, where the nets are selected manually from real crystal structures.

Recently, Blatov (2006*a*) proposed an algorithm for systematic generation of crystal-structure representations as subgraphs of the labelled quotient graph of an initial crystal structure. In this procedure, the 'significant' representations are chosen by some chemical property, in particular, by the strength of interatomic bonds. The algorithm was implemented into the program package *TOPOS* (Blatov, 2006*a*,*b*) to process crystal structures of any complexity. When analysing abstract periodic nets, one should replace this criterion with a more formal one; it seems reasonable to consider the net *simplicity* or high symmetry (Ockwig *et al.*, 2005) as such a criterion. In this paper, we unite the labelled-quotient-graph description of the net, the group–subgroup method of searching for net relations and the computer tools for generating crystal-structure representations to derive all uninodal subnets for all RCSR uninodal nets and sphere packings and to find the pathways of their mutual transformations.

2. The method to search for topological relations between nets

Below we study only ***three-dimensional*** periodic uninodal nets, including interpenetrating arrays of equivalent nets. However, the method described can easily be applied to nets with any prescribed finite number of inequivalent nodes; no special improvement is required. Any node degree (coordination number) is allowed, but for the uninodal nets collected in RCSR the maximal node degree is 16 (**dia-x**); for sphere packings, evidently, it does not exceed 12.

[4] *TOPOS* Topological Database, http://www.topos.ssu.samara.ru.

2.1. Generating subnets

To produce all uninodal subnets of a given net, we use the following two-step procedure.

(i) Let us consider a three-dimensional periodic net A (***supernet***) whose most symmetrical Euclidean ***embedding*** corresponds to a space group G. Note that the intrinsic symmetry of the net may be higher than G, we are not limited to only *crystallographic* nets, for which the automorphism group must be isomorphic to G (Klee, 2004). Moreover, the net may be not single, *i.e.* a set of equivalent interpenetrating nets may exist. To derive a three-dimensional periodic subnet $S(A)$, we should remove some edges from A keeping the three-dimensional periodicity. If we hold the space group, this is possible only if there are at least two kinds of edges, *i.e.* the initial net is not edge-transitive. If the number of inequivalent edges is higher than 1, the edges may be broken in m ways ($m > 1$). As a result, A can transform again to a single three-dimensional periodic net, to a set of interpenetrating three-dimensional periodic nets or to nets with a decreased dimensionality depending on the symmetry group of $S(A)$ (*cf.* Koch *et al.*, 2006). In general, not all the m ways give subnets of different topology, especially if A is highly symmetrical. All symmetrically and topologically inequivalent three-dimensional subnets generated at this step together with the initial net form a set of nets for further generation.

(ii) For each net from the set, all variants of decreasing its symmetry are considered that keep the given number of inequivalent nodes, for instance, retain the single inequivalent node in the case of uninodal nets. In general, all non-isomorphic translation-equivalent and class-equivalent maximal subgroups as well as isomorphic subgroups with enlarged unit cell (*International Tables for Crystallography*, 2004) should be considered for G. For each uninodal net with decreased symmetry generated at this step, the procedure is repeated starting from the first step until no subnet with new topology is found at the first step or no uninodal net with decreased symmetry is obtained at the second step.

All initial nets taken from RCSR or from the data on sphere packings are already represented in the most symmetrical embedding. To find such embeddings for new nets generated in this work, we have used the *Gavrog Systre* program (http://gavrog.org). To test the subnets for isomorphism, three topological indices have been applied: (i) ***coordination sequence*** $\{N_k\}$; in our study, k = 1–10, *i.e.* the first ten coordination shells are considered; (ii) ***extended Schläfli symbol*** collecting the size and number of shortest ***circuits*** in the net; (iii) ***vertex symbol*** that extracts ***rings*** from Schläfli symbols. The subnets are assumed isomorphic if they have all the indices equivalent. Note that RCSR and sphere-packing lists contain five pairs of nets, **lcv-f** (3/4/*c*7)–**sin** (3/4/*c*6), **noy** (5/4/*o*1)–**zfd** (5/4/*t*17), **srs-f** (5/3/*c*30)–**srs-g** (5/3/*c*31), **svp** (7/3/*t*13)–7/3/*o*2 and **wgy** (6/3/*t*11)–6/3/*o*2, with equal coordination sequences and extended Schläfli symbols, and one pair, **sxb**–**sxc**, with equal coordination sequences and vertex symbols, but all three indices distinguish these nets. In comparison with a stricter approach used in *Gavrog Systre*

Table 1
Low-symmetrical uninodal nets and subnets derived from the **qtz** and **tcb** topological types.

No.	Transformation sequence and resulting space group†	Number of inequivalent edges	Number of subnets	Subnet dimensionality and topology
	qtz			
1	$P6_222 \rightarrow \boldsymbol{P6_122}$ (**a**, **b**, 2**c**; 0, 0, 1/2)	1	0	
2	$P6_222 \rightarrow \boldsymbol{P6_2}$	1	0	
3	$P6_222 \rightarrow \boldsymbol{P3_221}$ (0, 0, 1/3)	1	0	
4	$P6_222 \rightarrow \boldsymbol{P6_422}$ (**a**, **b**, 2**c**; 0, 0, 1/2)	2	2	Array of one-dimensional chains {[100], [010], [110]}
5	$P6_222 \rightarrow \boldsymbol{P6_122}$ (**a**, **b**, 2**c**)	2	2	One-dimensional chains [001]
6	$P6_222 \rightarrow P6_122$ (**a**, **b**, 2**c**; 0, 0, 1/2) $\rightarrow \boldsymbol{P6_1}$	2	2	One-dimensional chains [001]
7	$P6_222 \rightarrow \boldsymbol{P6_1}$ (**a**, **b**, 2**c**)	2	2	One-dimensional chains [001]
8	$P6_222 \rightarrow \boldsymbol{P3_212}$ (0, 0, 1/6)	2	2	One-dimensional chains [001]
9	$P6_222 \rightarrow P3_221$ (0, 0, 1/3) $\rightarrow \boldsymbol{P3_121}$ (**a**, **b**, 2**c**; 0, 0, 1/2)	2	2	Array of one-dimensional chains {[100], [010], [110]}
10	$P6_222 \rightarrow P6_2 \rightarrow \boldsymbol{P3_2}$	2	2	One-dimensional chains [001]
11	$P6_222 \rightarrow P3_221$ (0, 0, 1/3) $\rightarrow \boldsymbol{P3_2}$	2	2	One-dimensional chains [001]
12	$P6_222 \rightarrow P3_212$ (0, 0, 1/6) $\rightarrow \boldsymbol{P3_2}$	2	2	One-dimensional chains [001]
13	$P6_222 \rightarrow P6_422$ (**a**, **b**, 2**c**; 0, 0, 1/2) $\rightarrow \boldsymbol{P6_522}$ (**a**, **b**, 2**c**)	3	6	Two cases of three-dimensional **bto** Two cases of array of one-dimensional chains {[100], [010], [110]} Two cases of zero-dimensional dimers
14	$P6_222 \rightarrow P3_212$ (0, 0, 1/6) $\rightarrow \boldsymbol{P3_112}$ (**a**, **b**, 2**c**)	4	14	Four cases of three-dimensional **bto** Two cases of array of one-dimensional chains {[100], [010], [110]} Four cases of one-dimensional chains [001] Four cases of zero-dimensional dimers
	tcb			
1	***Pnna***	2	2	Array of one-dimensional chains {[011], [01$\bar{1}$]}
2	$Pnna \rightarrow \boldsymbol{Pna2_1}$ (**a**, −**c**, **b**; 1/4, 0, 1/4)	2	2	Array of one-dimensional chains {[120], [1$\bar{2}$0]}
3	$Pnna \rightarrow \boldsymbol{Pnn2}$ (1/4, 0, 0)	3	6	Two cases of array of two interpenetrating three-dimensional **ths** (Class Ia) Array of one-dimensional chains {[011], [01$\bar{1}$]} Array of one-dimensional chains {[120], [1$\bar{2}$0]} Two cases of zero-dimensional dimers
4	$Pnna \rightarrow \boldsymbol{Pnc2}$ (**b**, **c**, **a**; 0, 1/4, 1/4)	3	6	Two cases of array of four interpenetrating three-dimensional **ths** (Class Ia) Array of one-dimensional chains {[011], [01$\bar{1}$]} Array of one-dimensional chains {[120], [1$\bar{2}$0]} Two cases of zero-dimensional dimers
5	$Pnna \rightarrow \boldsymbol{P222_1}$ (**c**, **a**, **b**; 1/4, 0, 1/4)	4	14	Two cases of double-deck layers (100) Two cases of double-deck layers (010) Two cases of array of three stranded one-dimensional helices [003] Array of one-dimensional chains {[101], [10$\bar{1}$]} Array of one-dimensional chains {[012], [01$\bar{2}$]} Two cases of one-dimensional chains [001] Four cases of zero-dimensional dimers

† All basis transformations and origin shifts are given with reference to the basis of a previous space group in the sequence. The resulting space group is bold. Only one possible transformation chain resulting in a given space group is shown.

(Delgado-Friedrichs & O'Keeffe, 2003), the method of topological indices is more universal because it allows one to work with non-crystallographic nets and crystallographic nets with collisions.

Example 1. The quartz topological type (**qtz**, 4/6/*h*1) has the most symmetrical embedding in the space group $P6_222$; the net is uninodal and edge-transitive. Therefore, the subnets with non-trivial topology can be obtained merely by decreasing the symmetry of the net. Only 14 low-symmetrical uninodal nets of the same topology may be generated by group–subgroup relations (Table 1). Nets Nos. 6, 7 and 10, 11, 12 differ only by origin shift and give rise to the same topological types of subnets, and nets Nos. 1, 2 and 3 are still edge-transitive and have no non-trivial subnets at a given symmetry. In most cases, the subnets are not three-periodic; only six ways of breaking one edge in nets Nos. 13 and 14 give rise to the single 3-coordinated three-dimensional periodic subnet **bto** (3/10/*h*1). Thus, **bto** is the only uninodal three-dimensional periodic subnet of **qtz**.

Example 2. Another 4-coordinated uninodal net **tcb** with highest symmetry *Pnna* is not a sphere packing and has two kinds of edges. Hence the subnets can be derived even at the highest symmetry but they are one-dimensional (Table 1; net No. 1). There are only two kinds of three-dimensional subnets in this case (Nos. 3 and 4) and both of them consist of interpenetrating arrays of two or four 3-coordinated **ths** (3/10/*t*4) nets. Besides, Table 1 contains interesting information about low-dimensional subnets of **tcb**, in particular, about triple-stranded one-dimensional helices (net No. 5), however, such cases lie beyond the scope of the paper.

The procedure described above was implemented into the program package *TOPOS* and enables one to derive all

Table 2
The number of investigated uninodal three-dimensional periodic nets.

Node degree	Number of initial nets	Number of generated subnets with novel topology	Node degree	Number of initial nets	Number of generated subnets with novel topology
3	–	31	8	47	722
4	232	452	9	18	389
5	266	1111	10	16	140
6	222	1314	11	7	39
7	112	1080	12	4	–

Table 3
EPINET nets found among the subnets generated.

Node degree	Net name†
4	*sqc*2075, *sqc*8109
5	*sqc*492, *sqc*498, *sqc*500, *sqc*3255, *sqc*3580, *sqc*3588, *sqc*7318, *sqc*9679
6	*sqc*24, *sqc*780, *sqc*911, *sqc*2969, *sqc*5167, *sqc*5184, *sqc*5323, *sqc*9035
8	*sqc*2, *sqc*117, *sqc*166, *sqc*876, *sqc*1653, *sqc*1878, *sqc*1909, *sqc*5117
9	*sqc*8843

† Only EPINET nets are listed that are inequivalent to the RCSR nets.

non-isomorphic subnets with a finite number of inequivalent nodes for a given set of nets.

2.2. Net relation graph

When all subnets $\{S(A_i)\}$ are obtained for a given set of supernets $\{A_i\}$, one can unite them into the same set $\{B_i\}$ = $\{A_i\}$ + $\{S(A_i)\}$, find the nets relating to each B_i and represent this information as a graph. The graph vertices correspond to the nets B_i, while the graph edges establish the supernet–subnet relations B_i–B_j, therefore we will call it a ***net relation graph*** (NRG). Thus, the NRG shown in Fig. 1 is derived from three supernets ($\{A_i\}$ = $\{B_1, B_2, B_3\}$) that have in total six subnets ($\{S(A_i)\}$ = $\{B_4, B_5, B_6, B_7, B_8, B_9\}$). Note that, if we restrict the number of nets and their subnets, for instance, considering only uninodal nets, the relation B_i–B_j–B_k does not mean that the direct relation B_i–B_k necessary exists. Indeed, the most symmetrical embedding of the intermediate net B_j may have a higher symmetry than the embedding of the corresponding subnet of B_i (examples are given in §3.1). In this case, the transition $B_i \rightarrow B_k$ can lead to an increase of the number of inequivalent nodes, and the space group of a uninodal embedding of B_k is not necessarily a subgroup of the space group of B_i. Thus, the net B_7 is a uninodal subnet both of B_1 and of B_4, whereas B_8 can be obtained from B_1 only through the intermediate subnet B_4 (Fig. 1) after an appropriate increase of its space-group symmetry. The following NRG properties are evident.

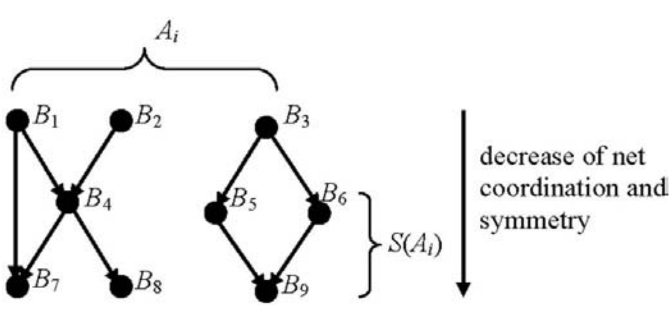

Figure 1
Net relation graph consisting of nine nets $\{B_i\}$, i = 1–9. The graph is generated from three initial supernets A_i = $\{B_1, B_2, B_3\}$ by successively deriving their subnets $S(A_i)$ = $\{B_4, B_5, B_6, B_7, B_8, B_9\}$.

(i) The *degree* of an ith NRG vertex, B_i, or NRG degree of the corresponding net, is equal to the number of nets B_j *adjacent* to the net B_i, *i.e.* transformable to B_i by adding/removing sets of equivalent edges to/from B_i. The set of adjacent nets may contain both supernets and subnets of B_i, which may have higher or lower space-group symmetry. For instance, the net B_4 (Fig. 1) has four adjacent nets; B_1 and B_2 are its supernets, whereas B_7 and B_8 are subnets.

(ii) The *path* B_i–B_j–...–B_k corresponds to a sequence of transformations that relate the nets B_i and B_k. The shortest path(s) B_i–...–B_k indicate the fastest way(s) of mutual transformations of B_i and B_k. Thus, the net B_4 is related to B_2 and B_8 only by the shortest (one-step) path (Fig. 1), whereas any adjacent pair of nets in the right part, say B_5 and B_9, can be transformed to each other both in one step and in three steps.

(iii) The *distance* between B_i and B_k, $d(B_iB_k)$, is equal to the number of transformations in the shortest path between B_i and B_k. If $d(B_iB_k) = \infty$, there is no path between B_i and B_k, and the corresponding nets cannot be transformed into each other through the nets of the NRG. For instance, $d(B_4B_k) = 1$ for k = 1, 2, 7, 8 and $d(B_4B_k) = \infty$ for k = 3, 5, 6, 9 (Fig. 1).

(iv) The *adjacency sequence* of B_i, $\{N_k(B_i)\}$, k = 1–n, is a set of numbers of nets B_j with $d(B_iB_j) = k$. Thus, the notion of adjacency sequence is similar to the notion of coordination sequence if one compares NRG and a net as abstract graphs. N_1 is equal to the NRG degree of B_i: $\sum_k N_k = N$, where N is the number of vertices in the connected part of NRG containing B_i. n is the length of the adjacency sequence; it shows how many transformation steps are required to generate all nets within the connected part of NRG starting from B_i. The key role of the net B_4 is evident in the left part of the NRG (Fig. 1): its adjacency sequence {4} has the smallest n = 1, *i.e.* any net in this part may be generated from B_4 in one step.

(v) If *NRG* consists of l parts, then there are l sets of nets, such that $d(B_iB_j) = \infty$ if and only if B_i and B_j belong to different sets. The NRG in Fig. 1 consists of two parts; the nets B_1, B_2, B_4, B_7 and B_8 are topologically independent of the nets B_3, B_5, B_6 and B_9.

Table 4
New homogeneous sphere packings derived from uninodal nets.

Initial net	Transformation sequence and resulting space group†	Node degree	Net name	**a** (Å) *x*	**b** (Å) / *β* (°) *y*	**c** (Å) *z*
uke	***Fddd***	3	**uke**-3-*Fddd*	5.250 0.3093	1.731 0.0842	6.087 0.0437
bct	*I4/mmm* → $P4_2/mmc$ (0, 1/2, 0) → $P4_2/nnm$ (**a**−**b**, **a**+**b**, **c**; 1/2, 0, 0) → *Pnnn* → ***Fddd*** (2**a**, 2**b**, 2**c**)	4	**bct**-4-*Fddd*	3.572 0.2589	6.097 0.3070	1.700 0.2106
fnl	$I4_1/amd$ → ***Fddd*** (**a**−**b**, **a**+**b**, **c**; 1/4, 3/4, 1/4)	4	**fnl**-4-*Fddd*	2.589 0.0173	3.012 0.4872	7.292 0.0681
acs	$P6_3/mmc$ → $P\bar{3}m1$ → *C2/m* (−**a**+**b**, −**a**−**b**, **c**) → ***C2/c*** (**a**, **b**, 2**c**)	5	**acs**-5-*C2/c*	2.445 0.3438	1.600 / 102.6 0.3750	2.400 0.3542
bct	*I4/mmm* → $P4_2/mmc$ (0, 1/2, 0) → $P4_2/nnm$ (**a**−**b**, **a**+**b**, **c**; 1/2, 0, 0) → *Pnnn* → ***Fddd*** (2**a**, 2**b**, 2**c**)	5	**bct**-5-*Fddd*-1	2.872 0.3340	5.404 0.0344	2.353 0.0815
bct	*I4/mmm* → $P4_2/mmc$ (0, 1/2, 0) → $P4_2/nnm$ (**a**−**b**, **a**+**b**, **c**; 1/2, 0, 0) → *Pnnn* → ***Fddd*** (2**a**, 2**b**, 2**c**)	5	**bct**-5-*Fddd*-2	1.595 0.2500	3.668 0.2500	6.080 0.2996
bsn	$I4_1/amd$ → *Imma* → *C2/m* (−**a**−**c**, **b**, **a**; 1/4, 1/4, 1/4) → ***C2/c*** (**a**, **b**, 2**c**)	5	**bsn**-5-*C2/c*	2.061 0.4002	2.779 / 154.0 0.4230	3.739 0.0690
nce	*I4/mmm* → *Immm* → *Pnnn* (1/4, 1/4, 1/4) → ***Fddd*** (2**a**, 2**b**, 2**c**; 1/2, 0, 0)	5	**nce**-5-*Fddd*-1	1.668 0.1250	3.104 0.4639	7.524 0.0585
nce	*I4/mmm* → *Immm* → *Pnnn* (1/4, 1/4, 1/4) → ***Fddd*** (2**a**, 2**b**, 2**c**; 1/2, 0, 0)	5	**nce**-5-*Fddd*-2	1.785 0.3750	6.977 0.1890	2.903 0.0473
nce	*I4/mmm* → *Fmmm* (**a**−**b**, **a**+**b**, **c**) → *Cmme* (**c**, **a**, **b**; 1/4, 1/4, 0) → ***Ccce*** (**a**, **b**, 2**c**; 1/4, 1/4, 0)	5	**nce**-5-*Ccce*	2.265 0.3439	3.224 0.1403	2.543 0.1110
snp	$P4_2/mmc$ → *Cccm* (**a**−**b**, **a**+**b**, **c**) → ***C2/c***	5	**snp**-5-*C2/c*	3.002 0.3603	2.487 / 101.7 0.0970	1.752 0.0383
snw	$I4_1/amd$ → *Fddd* (**a**−**b**, **a**+**b**, **c**; 1/4, 3/4, 1/4) → ***Fdd2*** (**c**, **a**, **b**; 3/8, 0, 3/8)	5	**snw**-5-*Fdd2*	2.443 0.1787	4.684 0.0521	1.601 0.4891
sxb	*Cccm* → *Pnnn* (1/4, 1/4, 0) → ***Fddd*** (2**a**, 2**b**, 2**c**; 1/2, 0, 1/2)	5	**sxb**-5-*Fddd*	1.787 0.3750	3.787 0.0070	5.367 0.0832
wfl	$I4_1/amd$ → ***Fddd*** (**a**−**b**, **a**+**b**, **c**; 1/4, 3/4, 1/4)	5	**wfl**-5-*Fddd*	5.417 0.0340	2.316 0.3372	2.903 0.0933
wfm	$I4_1/amd$ → ***Fddd*** (**a**−**b**, **a**+**b**, **c**; 1/4, 3/4, 1/4)	5	**wfm**-5-*Fddd*	2.809 0.3485	5.346 0.0341	2.446 0.0771
xfc	$I4_1/amd$ → ***Fddd*** (**a**−**b**, **a**+**b**, **c**; 1/4, 3/4, 1/4)	5	**xfc**-5-*Fddd*	5.314 0.0326	2.741 0.1593	2.562 0.4333
6/4/*t*7	*I4/mmm* → *Fmmm* (**a**−**b**, **a**+**b**, **c**) → ***Ccce*** (**c**, **a**, **b**; 1/4, 1/4, 0)	5	6/4/*t*7-5-*Ccce*-1	3.615 0.1329	1.618 0.3357	3.097 0.0948
6/4/*t*7	*I4/mmm* → *Fmmm* (**a**−**b**, **a**+**b**, **c**) → ***Cmce***(−**b**, **a**, **c**)	5	6/4/*t*7-5-*Cmce*	3.786 0.3679	3.003 0.1547	1.640 0.1127
bct	*I4/mmm* → $P4_2/mmc$ (0, 1/2, 0) → $P4_2/nnm$ (**a**−**b**, **a**+**b**, **c**; 1/2, 0, 0) → *Pnnn* → ***Fddd*** (2**a**, 2**b**, 2**c**)	6	**bct**-6-*Fddd*	5.490 0.0375	2.368 0.0662	2.770 0.2984
eca	$P6_3/mmc$ → $P\bar{3}m1$ → *C2/m* (−**a**+**b**, −**a**−**b**, **c**) → ***C2/c*** (**a**, **b**, 2**c**)	6	**eca**-6-*C2/c*	2.952 0.1721	1.705 / 100.1 0.0863	1.911 0.2970
ecl	*I4/mmm* → *Fmmm* (**a**−**b**, **a**+**b**, **c**) → ***Cccm*** (**c**, **a**, **b**; 1/4, 0, 1/4)	6	**ecl**-6-*Cccm*	3.860 0.3724	1.000 0.0893	3.970 0.3740
ecu	*Cmcm* → *Pbcm* (1/4, 1/4, 0) → ***Pbcn*** (**c**, 2**a**, **b**)	6	**ecu**-6-*Pbcn*	1.634 0.3750	1.826 0.2999	2.920 0.4063
ecu	*Cmcm* → $P2_1/m$ (1/2**a**+1/2**b**, **c**, 1/2**a**−1/2**b**) → $\boldsymbol{P2_1/c}$ (**a**, **b**, 2**c**)	6	**ecu**-6-$P2_1/c$	1.632 0.4385	1.634 / 146.3 0.3752	2.945 0.1255
hex	*P6/mmm* → *Cmmm* (−**a**+**b**, −**a**−**b**, **c**) → *Pban* (1/4, 1/4, 0) → *Pnnn* (**a**, **b**, 2**c**; 0, 0, 1/2) → ***Fddd*** (2**a**, 2**b**, 2**c**; 1/2, 0, 0)	6	**hex**-6-*Fddd*	2.369 0.0817	3.916 0.0000	3.223 0.3437
hex	*P6/mmm* → *Cmmm* (−**a**+**b**, −**a**−**b**, **c**) → *Pmma* (**a**, −**c**, **b**; 1/4, 1/4, 0) → $P222_1$ (**b**, **c**, **a**) → $\boldsymbol{C222_1}$ (2**a**, 2**b**, **c**)	6	**hex**-6-$C222_1$	1.823 0.1842	2.739 0.3196	1.786 0.4574
hex	*P6/mmm* → *Cmmm* (−**a**+**b**, −**a**−**b**, **c**) → *Pmma* (**a**, −**c**, **b**; 1/4, 1/4, 0) → *Cmce* (2**b**, 2**c**, **a**) → ***C2/m*** (−**b**, **a**, **c**)	6	**hex**-6-*C2/m*	1.860 0.3054	2.736 / 102.4 0.3172	1.816 0.2622
nce	*I4/mmm* → *Immm* → *Pnnn* (1/4, 1/4, 1/4) → ***Fddd*** (2**a**, 2**b**, 2**c**; 1/2, 0, 0)	6	**nce**-6-*Fddd*	5.589 0.2914	2.355 0.1766	2.651 0.3079
nce	*I4/mmm* → *Fmmm* (**a**−**b**, **a**+**b**, **c**) → *Cmme* (**c**, **a**, **b**; 1/4, 1/4, 0) → ***Ibca*** (**a**, **b**, 2**c**)	6	**nce**-6-*Ibca*	2.752 0.4206	3.462 0.1201	1.799 0.0955
nce	*I4/mmm* → *Fmmm* (**a**−**b**, **a**+**b**, **c**) → *Cmme* (**c**, **a**, **b**; 1/4, 1/4, 0) → ***Ccce*** (**a**, **b**, 2**c**; 1/4, 1/4, 0)	6	**nce**-6-*Ccce*	3.546 0.1160	1.760 0.0886	2.596 0.0915
nce	*I4/mmm* → *Fmmm* (**a**−**b**, **a**+**b**, **c**) → *Cmme* (**c**, **a**, **b**; 1/4, 1/4, 0) → ***Cmce*** (**a**, **b**, 2**c**)	6	**nce**-6-*Cmce*	2.737 0.1827	1.859 0.3553	3.545 0.1189
nce	*I4/mmm* → *Fmmm* (**a**−**b**, **a**+**b**, **c**) → *Cmme* (**c**, **a**, **b**; 1/4, 1/4, 0) → ***Ibam*** (**b**, 2**c**, **a**)	6	**nce**-6-*Ibam*	2.527 0.1647	1.805 0.1535	3.665 0.3636
nce	*I4/mmm* → *Fmmm* (**a**−**b**, **a**+**b**, **c**) → *Cmce* (**a**, −**c**, **b**) → ***C2/c*** (1/4, 1/4, 0)	6	**nce**-6-*C2/c*	1.794 0.2279	2.897 / 100.2 0.0930	1.685 0.1169
nci	*Fmmm* → *Cmme* (**c**, **a**, **b**; 1/4, 1/4, 0) → ***Ccce*** (**a**, **b**, 2**c**; 1/4, 1/4, 0)	6	**nci**-6-*Ccce*	3.554 0.1188	2.410 0.0749	1.865 0.1063
ose	*Immm* → *Pmmn* (1/4, 1/4, 1/4) → ***Pccn*** (**a**, **b**, 2**c**)	6	**ose**-6-*Pccn*-1	1.000 0.3749	2.835 0.5792	3.196 0.1342
ose	*Immm* → *Pmmn* (**c**, **a**, **b**; 1/4, 1/4, 1/4) → ***Pccn*** (**a**, **b**, 2**c**)	6	**ose**-6-*Pccn*-2	2.841 0.5785	1.671 0.3170	1.949 0.1677

Table 4 (continued)

Initial net	Transformation sequence and resulting space group†	Node degree	Net name	**a** (Å) *x*	**b** (Å) / β (°) *y*	**c** (Å) *z*
ose	*Immm* → *C*2/*m* (−**b**+**c**, **a**, **b**) → ***C*2/*c*** (**a**, **b**, 2**c**)	6	**ose**-6-*C*2/*c*-1	1.826 0.0329	2.724 / 127.0 0.3188	2.244 0.0444
ose	*Immm* → *C*2/*m* (−**b**+**c**, **a**, **b**) → ***C*2/*c*** (**a**, **b**, 2**c**)	6	**ose**-6-*C*2/*c*-2	2.119 0.5658	2.838 / 127.9 0.1719	1.951 0.0439
ose	*Immm* → *C*2/*m* (−**a**−**b**, **c**, **b**) → ***C*2/*c*** (**a**, **b**, 2**c**)	6	**ose**-6-*C*2/*c*-3	3.130 0.1713	1.668 / 114.6 0.0668	1.950 0.6147
svf	*I*4/*mcm* → *Ibam* → ***Pbcn*** (−**b**, **a**, **c**)	6	**svf**-6-*Pbcn*	2.408 0.3497	2.367 0.1456	1.449 0.0119
svf	*I*4/*mcm* → *Ibam* → ***C*2/*c*** (**a**−**c**, **b**, **c**)	6	**svf**-6-*C*2/*c*	2.849 0.3502	2.364 / 122.1 0.3541	1.448 0.3548
svg	*I*4/*mmm* → *Fmmm* (**a**−**b**, **a**+**b**, **c**) → ***Ccce*** (**c**, **b**, −**a**; 1/4, 1/4, 0)	6	**svg**-6-*Ccce*	1.669 0.0704	3.545 0.1129	3.046 0.0905
svg	*I*4/*mmm* → *Fmmm* (**a**−**b**, **a**+**b**, **c**) → ***Cmce*** (−**b**, **a**, **c**)	6	**svg**-6-*Cmce*	3.623 0.3620	2.958 0.1626	1.712 0.0794
svg	*I*4/*mmm* → *Fmmm* (**a**−**b**, **a**+**b**, **c**) → ***Cmcm*** (**b**, **c**, **a**; 1/4, 0, 1/4)	6	**svg**-6-*Cmcm*	2.907 0.3280	1.782 0.3426	3.656 0.1132
wfm	$I4_1/amd$ → ***Fddd*** (**a**−**b**, **a**+**b**, **c**; 1/4, 3/4, 1/4)	6	**wfm**-6-*Fddd*	3.880 0.0020	3.068 0.3470	2.566 0.0670
bct	*I*4/*mmm* → *Fmmm* (**a**−**b**, **a**+**b**, **c**) → *Cmme* (**b**, **c**, **a**; 1/4, 0, 1/4) → ***Ibam*** (**b**, 2**c**, **a**)	7	**bct**-7-*Ibam*	1.833 0.3512	2.476 0.1692	1.676 0.0000
bct	*I*4/*mmm* → *Fmmm* (**a**−**b**, **a**+**b**, **c**) → *Cmme* (0, 1/4, 1/4) → *Ibam* (**b**, 2**c**, **a**) → ***C*2/*c*** (−**b**−**c**, **a**, **c**)	7	**bct**-7-*C*2/*c*	3.106 0.1609	1.666 / 142.0 0.1697	2.673 0.2499
eca	$P6_3/mmc$ → $P\bar{3}m1$ → *C*2/*m* (−**a**+**b**, −**a**−**b**, **c**) → ***C*2/*c*** (**a**, **b**, 2**c**)	7	**eca**-7-*C*2/*c*	2.694 0.3390	1.667 / 99.9 0.4194	1.927 0.3459
ecl	*I*4/*mmm* → *Fmmm* (**a**−**b**, **a**+**b**, **c**) → ***Ccce*** (**c**, **b**, −**a**; 1/4, 1/4, 0)	7	**ecl**-7-*Ccce*	3.859 0.1277	1.000 0.3351	3.703 0.1169
ecl	*I*4/*mmm* → *Fmmm* (**a**−**b**, **a**+**b**, **c**) → ***Cmce*** (−**b**, **a**, **c**)	7	**ecl**-7-*Cmce*	3.932 0.3729	3.673 0.1321	1.000 0.1210
ecu	*Cmcm* → *Pbcm* (1/4, 1/4, 0) → ***Pbca*** (2**a**, **b**, **c**)	7	**ecu**-7-*Pbca*	1.941 0.3383	2.697 0.3831	1.393 0.1637
ecu	*Cmcm* → *C*2/*m* (−**b**, **a**, **c**) → ***C*2/*c*** (**a**, **b**, 2**c**)	7	**ecu**-7-*C*2/*c*	2.687 0.1341	1.000 / 93.9 0.1232	2.690 0.1299
ecu	*Cmcm* → *C*2/*c* → $P2_1/c$ (1/4, 1/4, 0)	7	**ecu**-7-$P2_1/c$	1.000 0.1770	2.697 / 103.8 0.1169	1.392 0.2804
ele	***Fdd*2**	7	**ele**-7-*Fdd*2	2.691 0.1077	5.358 0.3100	1.000 0.0404
fcu	$Fm\bar{3}m$ → *I*4/*mmm* (1/2**a**−1/2**b**, 1/2**a**+1/2**b**, **c**) → $P4_2/nnm$ (1/4, 3/4, 1/4) → $I4_1/amd$ (**a**−**b**, **a**+**b**, 2**c**; 0,1/2,0) → *Fddd* (**a**−**b**, **a**+**b**, **c**; 1/4, 3/4, 1/4) → ***Fdd*2** (**b**, **c**, **a**; 0, 3/8, 3/8)	7	**fcu**-7-*Fdd*2	2.850 0.0833	3.519 0.2058	1.646 0.1931
hex	*P*6/*mmm* → *Cmmm* (−**a**+**b**, −**a**−**b**, **c**) → *Ibam* (**a**, **b**, 2**c**) → *Pbcm* (−**b**, **a**, **c**; 1/4, 1/4, 1/4) → *Pbca* (2**a**, **b**, **c**) → ***Cmce***‡	7	**hex**-7-*Cmce*-1	1.968 0.0000	1.968 0.1639	1.882 0.2970
hex	*P*6/*mmm* → *Cmmm* (−**a**+**b**, −**a**−**b**, **c**) → *Pmma* (**b**, **c**, **a**; 1/4, 1/4, 0) → *Pbcm* (**b**, 2**c**, **a**) → *Pbcn* (**c**, 2**a**, **b**) → ***Cmce***‡	7	**hex**-7-*Cmce*-2	1.967 0.0000	3.627 0.3694	1.000 0.3398
hex	*P*6/*mmm* → *Cmmm* (−**a**+**b**, −**a**−**b**, **c**) → *Imma* (**a**, −2**c**, **b**) → *C*2/*m* (−**b**−**c**, **a**, **c**) → ***C*2/*c*** (**a**, **b**, 2**c**)	7	**hex**-7-*C*2/*c*	2.202 0.2483	1.872 / 116.7 0.0436	1.973 0.1600
nce	*I*4/*mmm* → *Fmmm* (**a**−**b**, **a**+**b**, **c**) → ***Cmce*** (**a**, −**c**, **b**)	7	**nce**-7-*Cmce*	1.646 0.0000	2.850 0.3333	1.760 0.4114
nce	*I*4/*mmm* → *Fmmm* (**a**−**b**, **a**+**b**, **c**) → *Cmce* (**a**, −**c**, **b**) → ***C*2/*c*** (1/4, 1/4, 0)	7	**nce**-7-*C*2/*c*	1.782 0.2086	3.317 / 108.0 0.1066	1.414 0.0811
nci	*Fmmm* → *Cmme* (**c**, **a**, **b**; 1/4, 1/4, 0) → ***Ccce*** (**a**, **b**, 2**c**; 1/4, 1/4, 0)	7	**nci**-7-*Ccce*	1.911 0.1917	3.808 0.3720	1.950 0.0755
nci	*Fmmm* → *Cmme* (**c**, **a**, **b**; 1/4, 1/4, 0) → ***Cmce*** (**a**, **b**, 2**c**)	7	**nci**-7-*Cmce*	3.955 0.1264	1.955 0.3282	1.904 0.3055
nci	*Fmmm* → *Cmme* (**c**, **a**, **b**; 1/4, 1/4, 0) → ***C*2/*m*** (−**b**, **a**, **c**)	7	**nci**-7-*C*2/*m*	1.955 0.2673	3.955 / 107.8 0.1264	1.000 0.1107
tsi	$I4_1/amd$ → *Imma* → *C*2/*m* (−**a**−**c**, **b**, **a**; 1/4, 1/4, 1/4) → ***C*2/*c*** (**a**, **b**, 2**c**)	7	**tsi**-7-*C*2/*c*	3.733 0.3805	1.000 / 104.9 0.4183	1.973 0.0634
tsi	$I4_1/amd$ → *Fddd* (**a**−**b**, **a**+**b**, **c**; 1/4, 3/4, 1/4) → *C*2/*c* (−**c**, **b**, 1/2**a**+1/2**c**) → $P2_1/c$ (1/4, 1/4, 0)	7	**tsi**-7-$P2_1/c$	1.392 0.2662	1.393 / 104.4 0.3359	1.942 0.2968
bct	*I*4/*mmm* → *Immm* → *Pmmn* (1/4, 1/4, 1/4) → ***Pnma*** (2**c**, **b**, −**a**)	8	**bct**-8-*Pnma*	1.871 0.1785	1.309 0.2500	1.414 0.1252
bct	*I*4/*mmm* → *Fmmm* (**a**−**b**, **a**+**b**, **c**) → *Cmme* (0, 1/4, 1/4) → *Pcca* (**b**, **c**, **a**; 1/4, 1/4, 0) → ***Pbcn*** (2**b**, **c**, **a**)	8	**bct**-8-*Pbcn*	1.914 0.1732	1.912 0.3098	1.856 0.0483
bct	*I*4/*mmm* → *Fmmm* (**a**−**b**, **a**+**b**, **c**) → *Cmme* (0, 1/4, 1/4) → *Ibam* (**b**, 2**c**, **a**) → ***C*2/*c*** (−**b**−**c**, **a**, **c**)	8	**bct**-8-*C*2/*c*-1	2.429 0.1734	1.912 / 128.0 0.1900	1.856 0.1882
bct	*I*4/*mmm* → *Fmmm* (**a**−**b**, **a**+**b**, **c**) → *Cmcm* (−**b**, **a**, **c**; 1/4, 0, 1/4) → *C*2/*m* (−**b**, **a**, **c**) → ***C*2/*c*** (**a**, **b**, 2**c**)	8	**bct**-8-*C*2/*c*-2	1.920 0.2307	1.921 / 104.9 0.4352	1.937 0.1756
chb	*Cmcm* → *Pbcm* (1/4, 1/4, 0) → ***Pbcn*** (**c**, 2**a**, **b**)	8	**chb**-8-*Pbcn*	1.000 0.3750	1.937 0.3500	3.486 0.3889
chb	*Cmcm* → *C*2/*m* (−**b**, **a**, **c**) → ***C*2/*c*** (**a**, **b**, 2**c**)	8	**chb**-8-*C*2/*c*	3.605 0.3571	1.000 / 103.9 0.4291	1.980 0.1874

Table 4 (continued)

Initial net	Transformation sequence and resulting space group†	Node degree	Net name	**a** (Å) *x*	**b** (Å) / β (°) *y*	**c** (Å) *z*
feb	*Pnma* → ***P*2₁/*c*** (**b**, **c**, **a**)	8	**feb**-8-*P*2₁/*c*	1.000 0.1673	1.837 / 105.1 0.1663	1.903 0.3329
nce	*I*4/*mmm* → *Immm* → *C*2/*m* (−**a**−**c**, **b**, **a**) → ***C*2/*c*** (**a**, **b**, 2**c**)	8	**nce**-8-*C*2/*c*	3.633 0.1435	1.000 / 107.4 0.0504	1.990 0.5784
nci	*Fmmm* → *Cccm* (**c**, **a**, **b**; 1/4, 0, 1/4) → ***C*2/*c*** (−**b**, **a**, **c**)	8	**nci**-8-*C*2/*c*	1.902 0.2673	3.688 / 102.0 0.1174	1.000 0.4080
svi-x	*I*4/*mcm* → *Ibam* → ***Pbcn*** (−**b**, **a**, **c**)	8	**svi-x**-8-*Pbcn*	2.443 0.3362	1.814 0.1520	1.669 0.0704
svi-x	*I*4/*mcm* → *Ibam* → ***C*2/*c*** (**a**−**c**, **b**, **c**)	8	**svi-x**-8-*C*2/*c*	3.248 0.3364	1.813 / 131.1 0.3478	1.668 0.3607
tcd	*R*$\bar{3}$*m* → *C*2/*m* (−1/3**a**+1/3**b**−2/3**c**, −**a**−**b**, **c**) → ***P*2₁/*c*** (**c**, **b**, −**a**)	8	**tcd**-8-*P*2₁/*c*	1.838 0.3888	1.000 / 149.0 0.1247	3.571 0.0833
bct	*I*4/*mmm* → *Fmmm* (**a**−**b**, **a**+**b**, **c**) → *C*2/*m* (**a**, **b**, −1/2**a**+1/2**c**) → *P*2₁/*m* (**c**, **b**, −**a**; 1/4, 1/4, 0) → ***P*2₁/*c*** (**a**, **b**, 2**c**)	9	**bct**-9-*P*2₁/*c*	1.000 0.1976	1.911 / 150.8 0.1918	3.435 0.1745
cco	*Cmcm* → *C*2/*m* (−**b**, **a**, **c**) → ***C*2/*c*** (**a**, **b**, 2**c**)	9	**cco**-9-*C*2/*c*	1.518 0.1744	1.303 / 99.8 0.3754	3.284 0.1338
chb	*Cmcm* → *Pbcm* (1/4, 1/4, 0) → ***Pbca*** (2**a**, **b**, **c**)	9	**chb**-9-*Pbca*	1.977 0.3586	3.236 0.3838	1.000 0.1742
chb	*Cmcm* → *C*2/*m* (−**b**, **a**, **c**) → ***C*2/*c*** (**a**, **b**, 2**c**)	9	**chb**-9-*C*2/*c*-1	3.225 0.1340	1.000 / 92.3 0.0665	1.982 0.1318
chb	*Cmcm* → *C*2/*m* (−**b**, **a**, **c**) → ***C*2/*c*** (**a**−2**c**, **b**, 2**c**)	9	**chb**-9-*C*2/*c*-2	3.836 0.1340	1.000 / 122.9 0.0675	1.982 0.5180
elb	***Cmce***	9	**elb**-9-*Cmce*	1.192 0.0000	1.606 0.1939	3.171 0.3766
fcu	*Fm*$\bar{3}$*m* → *I*4/*mmm* (1/2**a**−1/2**b**, 1/2**a**+1/2**b**, **c**) → *Immm* → *Pmmn* (**b**, **c**, **a**; 1/4, 1/4, 1/4) → *P*2/*c* (**a**, **c**, −**a**−**b**) → ***P*2₁/*c*** (**a**, 2**b**, **c**)	9	**fcu**-9-*P*2₁/*c*	1.000 0.1371	1.930 / 106.9 0.1158	1.711 0.2733
gpu	*Fddd* → *C*2/*c* (−**b**, **a**, 1/2**b**+1/2**c**) → ***P*2₁/*c*** (1/4, 1/4, 0)	9	**gpu**-9-*P*2₁/*c*	1.674 0.2676	1.000 / 104.9 0.3259	1.977 0.3079
hcp	*P*6₃/*mmc* → *Cmcm* (−**a**−**b**, **a**−**b**, **c**) → *Pbcm* (1/4, 1/4, 0) → ***Pbca*** (2**a**, **b**, **c**)	9	**hcp**-9-*Pbca*	1.913 0.1814	1.930 0.1158	1.711 0.1650

† See footnote to Table 1. Refined unit-cell dimensions and node positions are obtained with *Gavrog Systre*. ‡ Final space group is obtained with *Gavrog Systre*.

3. Analysis of relations between uninodal three-dimensional periodic nets

Below, this approach is applied to 924 4–12-coordinated uninodal three-dimensional periodic nets taken from RCSR (release of November 2006) and all published lists of sphere packings of orthorhombic, trigonal, tetragonal, hexagonal and cubic crystal systems (Table 2). Only single (non-interpenetrating) nets were taken as initial (A_i) supernets, however, interpenetrating arrays may appear as subnets (B_i). The nets with a larger node degree were omitted because they are *a priori* not sphere packings and are related to well known topologically simpler nets, as a rule. Thus, there are merely two such uninodal nets in RCSR, with node degrees 14 (**bcu-x**) and 16 (**dia-x**), and they are extended from an 8-coordinated **bcu** (8/4/*c*1) and a 4-coordinated **dia** (4/6/*c*1) sphere packing, respectively, by uniting the first two coordination shells of nodes. With the program package *TOPOS*, all the supernet–subnet relations are found and only uninodal three-dimensional periodic subnets are considered. Obviously, 3-coordinated nets should not be taken as initial supernets A_i because their uninodal subnet is not three-periodic, however, the 3-coordinated nets may appear as subnets of the nets with a higher node degree (Table 2). In this connection, it should be noted that all 57 3-coordinated RCSR nets and sphere packings are included in the NRG as subnets of the initial 4–12-coordinated nets. As a result, the total NRG consists of 6528 topologically different 3–12-coordinated nets B_i.

3.1. New uninodal nets

The first important result is that many of the generated subnets have novel topologies not described in the databases on periodic nets RCSR and EPINET[5] or in the lists of sphere packings (Table 2). Moreover, the number of novel topologies (5278; six of them are found only in interpenetrating arrays of several equivalent nets)[6] is much larger than the number of initial nets. It is interesting that none of the new uninodal nets is edge-transitive. Note that the greatest project on enumeration of periodic nets, EPINET, has currently given only 215 3–12-coordinated uninodal nets (Hyde *et al.*, 2006), 117 of which are not collected in RCSR or in the lists of sphere packings. It is important that, unlike the algorithm used in this study, the EPINET nets are obtained from abstract two-dimensional hyperbolic tilings and can be considered as a 'random' set of periodic nets, whose topology is independent of any physical properties of substance. In this relation, it should be mentioned that only 27 out of the 117 novel

[5] Euclidean Patterns in Non-Euclidean Tilings, http://epinet.anu.edu.au/.
[6] The crystallographic data and topological indices for all new uninodal nets are available as *TOPOS* crystallographic and topological databases at http://www.topos.ssu.samara.ru.

uninodal EPINET nets are found among the generated subnets (Table 3). This confirms once again the fact that Nature prefers some nets and avoids other ones.

Since many initial supernets closely relate to real crystal structures, one may expect that their subnets could also be crystallochemically 'significant'. In this respect, it is noteworthy that many of them correspond to the sphere packings not described earlier. Thus, the 3-coordinated subnet derived from the net **uke** by removing one independent edge is a sphere packing (O'Keeffe, 2006) not presented in the list of 3-coordinated sphere packings by Koch & Fischer (1995). In Table 4, 85 nets corresponding to new homogeneous (with one kind of sphere) sphere packings are given. Below we will apply the symbol **s**-*d*-*G*-*n* for the new nets, where **s** coincides with a conventional name of the initial net, *d* is an integer equal to the degree of a node in the new net, *G* is the space group for the most symmetrical embedding of the new net, *n* (optional) is the ordinal number if there are several non-isomorphic nets with a given **s**-*d*-*G* set.

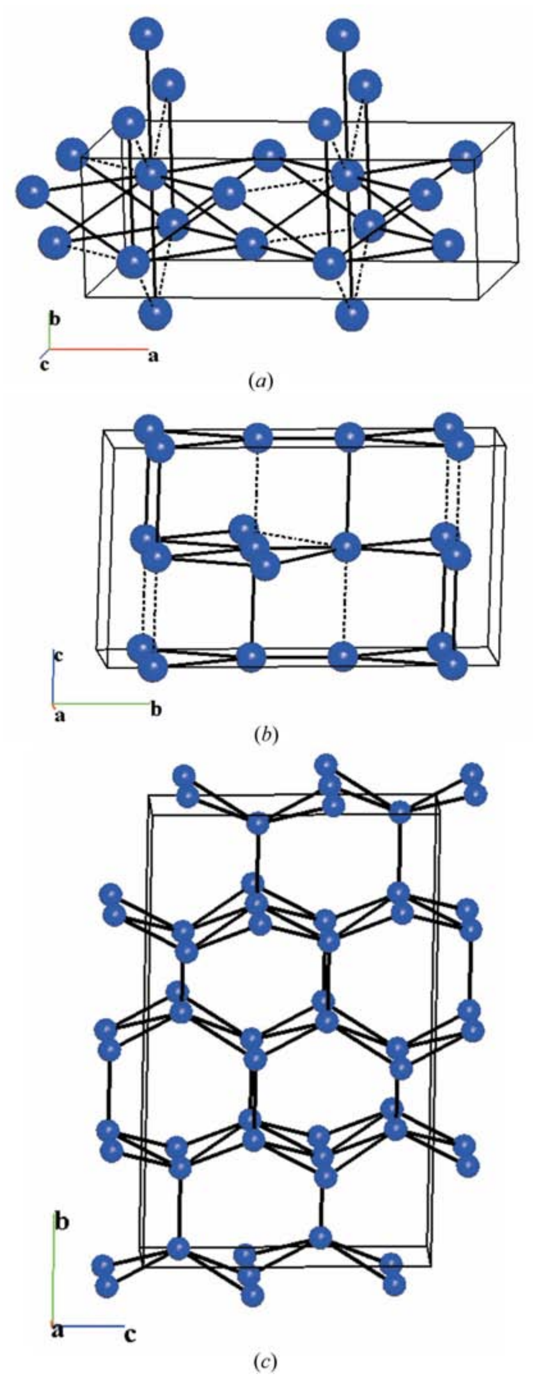

Figure 2
The main steps in generating an **hxg-d**-5-*Fddd* net from the **hxg-d** net. (*a*) Obtaining a 7-coordinated *Pcca* net; (*b*) obtaining a 5-coordinated *C*2/*c* net from the 7-coordinated *Pcca* net symmetrized up to *Cmmm*; (*c*) final 5-coordinated net symmetrized up to *Fddd*. The edges to be broken are dotted.

Examples. The last two nets in Table 5 are good examples to illustrate the algorithm of generating new nets. The symbol of the first of these nets, **hxg-d**-5-*Fddd*, means that it is derived from the 10-coordinated **hxg-d** net, is 5-coordinated, and its highest symmetry is *Fddd*. It is obtained in six steps: (i) decreasing the **hxg-d** symmetry by successive group–subgroup transformations, $Pn\bar{3}m \rightarrow P4_2/nnm\ (0, 1/2, 0) \rightarrow Cmme$ $(\mathbf{a}-\mathbf{b}, \mathbf{a}+\mathbf{b}, \mathbf{c}; 0, 1/2, 0) \rightarrow Pccm\ (\mathbf{b}, \mathbf{c}, \mathbf{a}) \rightarrow Pcca\ (2\mathbf{a}, \mathbf{b}, \mathbf{c})$; (ii) decreasing the node degree from ten to seven by removing three edges (Fig. 2*a*); (iii) finding the highest symmetry of the resulting 7-coordinated net ($Pcca \rightarrow Cmmm$) with the program *Gavrog Systre*; (iv) decreasing the symmetry according to the sequence $Cmmm \rightarrow C2/m \rightarrow C2/c\ (\mathbf{a}, \mathbf{b}, 2\mathbf{c})$; (v) decreasing the node degree from seven to five by removing two further edges (Fig. 2*b*); (vi) finding the highest symmetry of the resulting 5-coordinated net ($C2/c \rightarrow Fddd$; Fig. 2*c*). The latter net, *sqc*2-5-*C*2/*c*, is obtained from the 8-coordinated EPINET net *sqc*2 (*Pmmm*) by the following sequence: (i) the group–subgroup transformation of the initial net, $Pmmm \rightarrow Pccm\ (\mathbf{c}, \mathbf{a}, 2\mathbf{b}) \rightarrow Ccce\ (2\mathbf{a}, 2\mathbf{b}, \mathbf{c}) \rightarrow Pnna\ (-\mathbf{b}, \mathbf{a}, \mathbf{c};$ $1/4, 1/4, 0)$; (ii) decreasing the node degree from eight to six; (iii) finding the highest symmetry of the resulting 6-coordinated net ($Pnna \rightarrow P4/mmm$); (iv) decreasing the net symmetry by the transformations $P4/mmm \rightarrow Cmmm$ $(\mathbf{a}-\mathbf{b}, \mathbf{a}+\mathbf{b}, \mathbf{c}) \rightarrow C2/m \rightarrow C2/c\ (\mathbf{a}, \mathbf{b}, 2\mathbf{c})$; (v) decreasing the node degree from six to five; the resulting net has the highest possible symmetry. The nets **hxg-d**-5-*Fddd* and *sqc*2-5-*C*2/*c* relate to **dia** and **lon** nets as will be shown in §3.2.

Let us emphasize that the list of uninodal nets is not complete, but is *closed*, *i.e.* no uninodal subnet with new topology can be obtained from a net of the list and no new relations may be established between the nets of the NRG. However, a net may exist that is the supernet in relation to some nets listed. Anyway, such a net should not be crystallochemically 'significant' (see §3.3).

3.2. Transformation pathways between uninodal nets

The supernet–subnet relations enable one to find transformation pathways from one net to another as the paths in NRG. There are several advantages of this approach.

(i) Topologically, the fastest transformation, *i.e.* requiring the minimal number of acts of breaking or forming net edges, can be easily found corresponding to a shortest path of NRG.

(ii) Unlike all net–subnet transition mechanisms proposed earlier (Sowa & Koch, 2001, 2002) that take into account only the transformations with a decrease of node degree (through a subnet), the alternative pathways passing through a supernet may be considered. For instance, the nets B_5 and B_6 (Fig. 1) may be transformed to each other both through the subnet B_9 and through the supernet B_3. Although such mechanisms are not suitable for the nets, where the atoms have the largest possible coordination numbers, like polymorphs of carbon or silica considered in the papers cited, they may be important to describe transformations of the nets in more complicated compounds, in particular metal-organic substances, or to interpret pressure-induced phase transitions.

(iii) The transformation always passes through a common supernet or subnet, whose space group is a common supergroup or subgroup of the space groups of both initial nets. Therefore, the transformation is spatially continuous and requires the minimal number of acts to break existing bonds or to form new ones.

(iv) Using the net–subnet relations, one can find the transformation pathways with target interpenetrating arrays of uninodal nets. In this case, the initial structure may be a single net or also an interpenetrating array of nets of different topology or of the same topology and another number of nets in the array.

At the same time, the approach, being purely topological, gives no information about geometrical distortions of the nets and motion of atoms during the transition.

Example 1. Let us consider the possible transformation pathways for the nets of the diamond (**dia**, 4/6/*c*1) and the

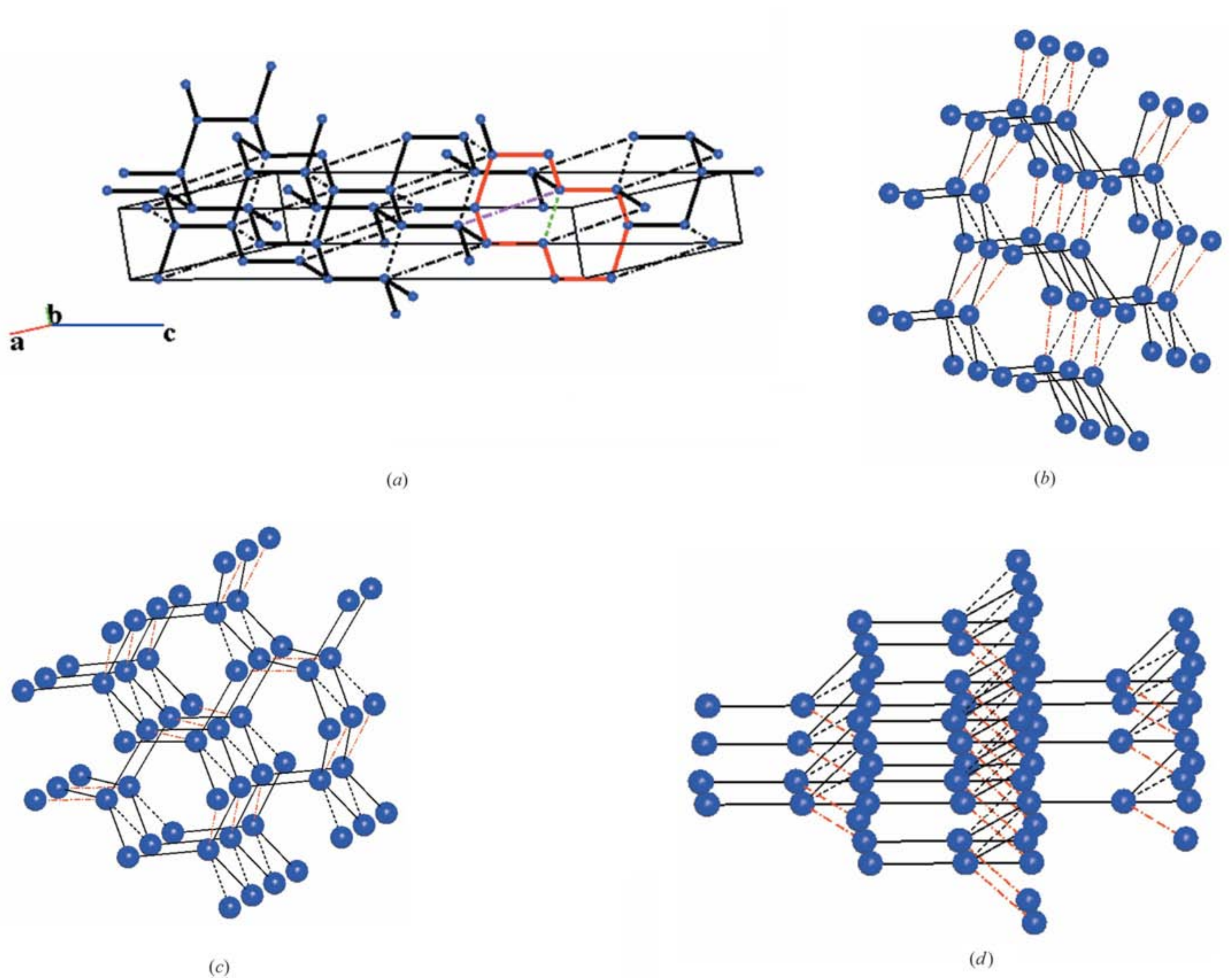

Figure 3
(*a*) Relations between **ths**, **sqp**, **dia** and **lon** nets. The intermediate **ths** net of the *C*2/*c* symmetry is shown by solid lines. Additional edges resulting in **dia** and **lon** nets are shown by dashed and dot-and-dashed lines, respectively. One of the dashed and one of the dot-and-dashed edges are coloured in green and magenta, respectively. One of the 10-rings in the **ths** net is red. The 5-coordinated net obtained from the **ths** net by adding both dashed and dot-and-dashed edges is **sqp**. (*b*) Relations between **hxg-d**-5-*Fddd*, **dia** and **lon** nets. (*c*) Relations between **noz**, **dia** and **lon** nets. (*d*) Relations between *sqc*2-5-*C*2/*c*, **dia** and **lon** nets. Breaking the red dot-and-dashed or the black dotted edges in the initial 5-coordinated net results in **dia** and **lon** nets, respectively.

Table 5
Possible transformation pathways from the diamond to the lonsdaleite topological type.

Transition net	Transformation pathway and resulting space group†
Subnet	
ths	**dia**: $Fd\bar{3}m \rightarrow R\bar{3}m$ (−1/2**a**+1/2**b**, −1/2**b**+1/2**c**, **a**+**b**+**c**)
	→ *C*2/*m* (−1/3**a**+1/3**b**−2/3**c**, −**a**−**b**, **c**) → ***C*2/*c*** (**a**, **b**, 2**c**)
	lon: $P6_3/mmc \rightarrow P\bar{3}1c$ → ***C*2/*c*** (−**a**−**b**, **a**−**b**, **c**)
Supernet	
noz	*Cmce* → ***Pbcn*** (**c**, **a**, **b**; 1/4, 1/4, 0) (**dia**)
	Cmce → $\boldsymbol{C222_1}$ (1/4, 0, 0) (**lon**)
sqp	*I*4/*mmm* → ***C*2/*c*** (**c**, **a**+**b**, −**a**+**b**; 1/2, 0, 0) (**dia**)
	*I*4/*mmm* → ***Cmcm*** (**a**−**b**, **a**+**b**, **c**; 1/4, 1/4, 1/4) (**lon**)
hxg-d-5-*Fddd*	*Fddd* → ***C*2/*c*** (−**b**, **a**, 1/2**b**+1/2**c**) (**dia**)
	Fddd → ***C*2/*c*** (**b**, **c**, 1/2**a**−1/2**b**; 0, 1/4, 1/4) (**lon**)
*sqc*2-5-*C*2/*c*	***C*2/*c*** (**dia**, **lon**)

† See footnote to Table 1.

Table 6
Possible transformation pathways resulting in twofold **ths** interpenetrating array.

Initial net	Transformation pathway and resulting space group†	Class of interpenetration
cds (4/6/*t*4)	$P4_2/mmc \rightarrow P\bar{4}2c$ (0, 0, 1/4) → $\boldsymbol{P\bar{4}n2}$ (**a**−**b**, **a**+**b**, **c**)	Ia
dmp	*Pnna* → ***Pnn*2** (1/4, 0, 0)	Ia
*sqc*2075	*I*4/*mcm* → *Ibam*	IIa
tcb	*Pnna* → ***Pnn*2** (1/4, 0, 0)	Ia
unm (4/6/*t*5)	$\boldsymbol{P4_22_12}$	Ia
upa (4/4/*t*11)	$\boldsymbol{P4_22_12}$	Ia
4/5/*t*2	$\boldsymbol{I\bar{4}2d}$	IIa

† See footnote to Table 1.

lonsdaleite (**lon**, 4/6/*h*2) topological types. Sowa & Koch (2001) proposed the only transition mechanism through a common 3-coordinated subnet **utp** (3/10/*o*1), whose space group (*Pnna*) is a common subgroup for the space groups of **dia** ($Fd\bar{3}m$) and **lon** ($P6_3/mmc$). However, according to Table 5, there is an additional transformation pathway through other 3-coordinated homogeneous sphere packings **ths** (3/10/*t*4, $I4_1/amd$) (Fig. 3*a*). Unlike the transition through **utp**, in this case the 3-coordinated net has a lower symmetry than the idealized sphere packing.

Moreover, the transformation pathways **dia** ↔ **lon** may pass through the nets with a higher node degree (supernets). Because the most symmetrical **dia** and **lon** embeddings have no common supergroup, in all the cases the nets have lower symmetries for which the space group of the supernet is a common supergroup. For this reason, any transition mechanism through a supernet may be applied only to the *topological* types **dia** and **lon**, where the space-group symmetry is not crucial, not to the diamond and the lonsdaleite *structure* types with a fixed (highest) spatial symmetry. There are in total 93 shortest (with one intermediate net) transformation pathways of this kind in the NRG; 23 of them include one of the initial RCSR nets and/or sphere packings: 5-coordinated **noz** (*Cmce*) and **sqp** (5/4/*t*6, *I*4/*mmm*); 6-coordinated **acs** (6/4/*h*2, $P6_3/mmc$), **pcu** (6/4/*c*1, $Pm\bar{3}m$) and **sxa** (*Cmme*); 7-coordinated 7/3/*m*1, **ose** (7/3/*o*5, *Immm*) and **sev** (7/4/*o*1, *Fmmm*); 8-coordinated **bcu** (8/4/*c*1, $Im\bar{3}m$), **eca** (8/3/*h*3, $P6_3/mmc$), **ecu** (8/3/*o*1, *Cmcm*), **hex** (8/3/*h*4, *P*6/*mmm*) and **osb** (8/3/*o*2, *Cmcm*); 9-coordinated **nce** (9/3/*t*2, *I*4/*mmm*) and **nci** (9/3/*o*1, *Fmmm*); 10-coordinated **bct** (10/3/*t*1, *I*4/*mmm*), **cco** (10/3/*o*1, *Cmcm*), **chb** (10/3/*o*2, *Cmcm*) and **tca** (10/3/*h*2, $P6_3/mmc$); 11-coordinated **elb** (*Cmce*) and **svi-x** (*I*4/*mcm*); 12-coordinated **fcu** (12/3/*c*1, $Fm\bar{3}m$) and **hcp** (12/3/*h*1, $P6_3/mmc$). Another 70 possible intermediate supernets are derived from **bcu**, **ecu**, **hex**, *sqc*2, **nce**, **bct**, **cco**, **chb**, **hxg-d**, **elb**, **svi-x**, **fcu** and **hcp**. In Table 5, only the 5-coordinated supernets are considered, including the new nets **hxg-d**-5-*Fddd* and *sqc*2-5-*C*2/*c*, which require the minimal number of new bonds to be formed during the transition (Figs. 3*a*–*d*). Note that **ths** and **sqp** nets correspond to the same topological motif, intermediate between **dia** and **lon** (Fig. 3*a*). Moreover, the **dia** and **lon** nets derived from *sqc*2-5-*C*2/*c* have the symmetry and unit cell of the initial net (Table 5), and the basic 3-coordinated net formed by solid edges in Fig. 3(*d*) is again **ths**.

Example 2. The interpenetrating array of two **ths** nets has one of the largest NRG degrees (814) among the interweaving motifs. This means that it can be derived from 814 topological types of nets with a higher node degree. However, only 51 cases correspond to 4-coordinated nets, *i.e.* require breaking merely one edge per node to give rise to the target **ths** array; seven of them are well known nets (Table 6; Figs. 4*a*–*g*). Note that in the last three cases in Table 6 the symmetries of supernet and subnet are the same. Moreover, corresponding lattice complexes are mentioned by Koch *et al.* (2006) as containing twofold interpenetrating sphere packings of two types: $t[3/10/t4]^2_{\rm I}$ and $t[3/10/t4]^2_{\rm II}$. This fact together with the data of Table 6 on classes of interpenetration (Blatov *et al.*, 2004) shows that different initial nets can give rise to different interpenetration modes of resulting arrays. Let us emphasize that the method described here allows one to find all interpenetrating motifs irrespective of their relation to sphere packings.

Example 3. The 6-coordinated net **roa** (*Cccm*) can be transformed to both twofold (*Pnn*2; Class Ia) and sixfold (*Fddd*; Class IIIa) **ths** interpenetrating arrays by the routes *Cccm* → *Ccc*2 → *Pnn*2 and *Cccm* → *Pnnn* (1/4, 1/4, 0) → *Fddd* (2**a**, 2**b**, 2**c**), respectively. Therefore, there is the transformation pathway twofold **ths** ↔ **roa** ↔ sixfold **ths** (Figs. 5*a*, *b*), moreover, according to the NRG, this is the only two-step pathway through a single net to increase the number of **ths** nets in the array up to six. Note that the example of a sixfold **ths** array was found in metal-organic compounds (ZIBRAD) with the same space group and class of interpenetration (Blatov *et al.*, 2004).

3.3. The graph of topological relations between uninodal nets

Among 6528 nets composing the NRG, there are 248 interpenetrating arrays with the number of single nets in the

Table 7
List of the *NRG* generators.

Node degree	Net name
4	**fau**, **kfi**, **lcv-a**, **mdf**, **tcb**, **ten**, **wse**
5	**fce**, **fch**, **fcl**, **fcm**, **fcn**, **fco**, **fda**, **fdc**, **fnn**, **lcy-a-x**, **srs-f**, **srs-g**, **wjk**, **wjm**, **wjn**, **wjq**, **wjr**, **wju**, **wjv**, **wjw**
6	**ana-e**, **nbo-f-z**, **pcu-m**, **roa**, **snb**, **snf**, **snh**, **snr**, **snv**, **sxi**, **sxm**, **sxn**, **sxo**, **sxp**, **twf-e**, **wgz**, **whe**, **who**, **whq**, **whs**, **wii**, **wij**, **wip**, **wiq**, **wir**, **wis**, **wit**, **wjb**, **wkj**, **wkk**, **wkl**, **wkm**, **wkn**, **wko**, **wkp**, **wkq**, **wkr**, **wks**, **wmd**, **wmp**, **wmq**, **wmt**, **wne**
7	7/3/*t*43, 7/3/*t*44, **gar-e**, **iac-e**, **ocu-e**, **sva**, **svm**, **svu**, **svv**, **svw**, **svx**, **svz**, **swa**, **swb**, **swe**, **swf**, **swh**, **toc-e**, **wfr**, **wfx**, **wjc**, **wkt**, **wku**, **wkv**, **wnh**, **wni**, **wnl**, **wnr**, **wnu**, **wnv**, **wnw**, **wnx**, **wny**, **xfa**, **xfi**, **xfj**, **xfk**, **xfl**, **xfm**, **xfn**, **xfo**, **xfp**, **xfq**, **xfr**, **xfs**
8	**bcs-e**, **ece**, **ech**, **eco**, **ecq**, **ecr**, **ecs**, **ect**, **ith-e**, **wfj**, **wfk**, **wfl**, **wfm**, **wfn**, **wfo**, **wfp**, **wkw**
9	**naz-x**, **nca**, **ncc**, **nck**, **thp-e**, **wal**, **wfc**
10	**hxg-d**, **lcw-x**, **tce**, **tch**, **tci**
11	**ele**, **elf**, **svi-x**
12	**fcu**, **hcp**, **nbo-x**, **thp-x**

Table 8
The single nets with a large NRG degree (>350).

Net	Node degree	NRG degree	Net	Node degree	NRG degree
fcu (12/3/*c*1)	12	2231	**nce** (9/3/*t*2)	9	496
fcu-11-$P4_2/mcm$	11	1149	**ths** (3/10/*t*4)	3	479
fcu-10-*Cmme*	10	839	**pcu** (6/4/*c*1)	6	442
hxg-d	10	780	**cds** (4/6/*t*4)	4	434
*sqc*2	8	771	**fcu**-10-$P4_222$	10	408
fcu-10-$P4_2/mmc$	10	721	**dia** (4/6/*c*1)	4	396
bct (10/3/*t*1)	10	642	**fcu**-9-*Pccm*-1	9	394
svi-x	11	614	**dia-f** (3/4/*t*1)	3	388
fcu-11-*Ibam*	11	539	**fcu**-9-*Pccm*-2	9	365
hcp (12/3/*h*1)	12	535	**sqp** (5/4/*t*6)	5	362
bnn (5/4/*h*5)	5	517			

array, Z, varying in the range 2–8. There are 197 arrays with $Z = 2$; 24 with $Z = 3$; 23 with $Z = 4$; two with $Z = 5$ [the single net topologies are **dia-a** (4/3/*c*6) and **dia-f** (3/4/*t*1)], one with $Z = 6$ (**ths**) and one with $Z = 8$ (**srs-a**, 3/3/*c*1). Note that the interpenetrating arrays were distinguished only by topology of the single net and Z, no other characteristics of interpenetration were considered (*cf.* Koch *et al.*, 2006). The NRG consists of two separate subgraphs; the main subgraph includes 6524 nets, it is analysed in detail below. The second subgraph includes only four nets: 3/8/*c*3, **rhr-a** (3/4/*c*9), **kfi** (4/4/*c*19, zeolite KFI) and **wse** (4/4/*c*18), which are related as shown in Fig. 6. This means that the four nets cannot be transformed to other nets through common 3–12-coordinated uninodal supernets or subnets. The nets that have no supernets in the NRG are of special interest; they can be considered as the NRG generators because all other nets can be obtained as their descendants (subnets). The number of such generators (151) is unexpectedly large; all of them are listed in Table 7.

Not all nets play the same role in the main subgraph; it is reasonable to arrange them according to their NRG degree. Obviously, the nets with a large NRG degree are important because they lie on many transformation pathways (*cf.* Fig. 1). It is not surprising that the first places are occupied by high-coordinated nets (with node degree 10–12) that have a large number of subnets (Table 8). However, not all high-coordinated nets are at the top of the list; the place evidently depends on the peculiarities of the net topology and symmetry. Thus, a face-centred cubic lattice (**fcu**) has NRG degree much larger than other nets, moreover, many leading nets are derived from **fcu**. Comparatively, the other uninodal close sphere packing, **hcp**, has a significantly smaller NRG degree. This fact probably explains why the **fcu** motif prevails over the **hcp** topology in the architecture of organic crystals (Peresypkina & Blatov, 2000).

Table 9
The nets with largest NRG degrees depending on node degree of the net.

Node degree	Net	NRG degree	MOFs†	Node degree	Net	NRG degree	MOFs†
3	**ths** (3/10/*t*4)	479	2	5	**bnn** (5/4/*h*5)	517	1
	dia-f (3/4/*t*1)	388			**sqp** (5/4/*t*6)	362	2
	dia-g (3/4/*t*2)	216			**sxa**-5-*Pccm*-1	272	
	utg (3/8/*t*5)	188			**sxa**-5-*Pccm*-2	270	
	srs (3/10/*c*1)	178	1		**sxa**-5-*Cmmm*	255	
	3/8/*t*6	168			5/4/*t*5	240	
	hxg-d-3-$I4_122$	146			6/4/*t*8-5-*Ibam*	238	
	pcu-h (3/6/*h*1)	131			**nov**	208	‡
	bto (3/10/*h*1)	113			**sxa**-5-*Ibam*	195	
	utp (3/10/*o*1)	104			**bct**-5-*Ibam*	181	
4	**cds** (4/6/*t*4)	434	4	6	**pcu** (6/4/*c*1)	442	1
	dia (4/6/*c*1)	396	1		**sxa**	287	
	4/4/*t*37	325			**msw**	229	
	irl (4/4/*o*2)	319	10		**svi-x**-6-$P4_2/mcm$	185	
	sra (4/4/*o*1)	300	2		**rob**	173	
	crb (4/4/*t*5)	254	5–7		**sxd** (6/3/*o*1)	159	
	lon (4/6/*h*2)	236	8–9		**hxg-d**-6-*Pccm*	153	
	sni-4-*P4/nbm*	234			**hxg-d**-6-*Cmmm*	151	
	neb (4/6/*o*1)	227			**hxg-d**-6-$P4_222$	145	
	4/4/*t*43	194			**snp** (6/3/*t*5)	136	

† Position in the list of occurrence of uninodal nets of a given coordination in metal-organic frameworks according to Ockwig *et al.* (2005). ‡ The number of cases is less than three.

For crystal chemistry, it is important to take into account the net coordination; the high-coordinated nets are rare in metal-organic frameworks due to rather low typical coordination numbers (3–6) of the metal centres. Some well known low-coordinated nets, such as **ths**, **dia**, **cds**, **pcu**, compete with the high-coordinated ones in the list of nets with large NRG degree (Table 8). In Table 9, for each node degree in the range 3–6, the top ten single nets are given; most of the nets were found in real crystal structures and have familiar RCSR names. In all cases, the top nets frequently occur in metal-organic frameworks according to Ockwig *et al.* (2005). However, the order of occurrence does not always coincide with the order of NRG degree. Obviously, other, not only topological, reasons should be taken into account; for instance, the tetrahedral coordination is more typical for the metal centres than the rectangular coordination and, as a result, the **dia** topology prevails over the **cds** topology in metal-organic frameworks. At the same time, according to

Table 9, some nets with a large NRG degree are not listed in RCSR; among them there are sphere packings 3/8/*t*6, 4/4/*t*37, 4/4/*t*43 and 5/4/*t*5.

For crystal design, it could be useful to know what kinds of interpenetration often occur in the net interrelations. Table 10 contains such information for 3- and 4-coordinated nets because they mostly form interpenetrating arrays. As for single nets, the interpenetrating arrays with a large NRG degree are frequent in metal-organic (Blatov *et al.*, 2004) and inorganic (Baburin *et al.*, 2005) crystals. Moreover, the topologies of the top single and interpenetrating nets are often the same (Tables 9, 10); this fact is especially interesting because they relate to quite different nets in the NRG. It is noteworthy that the top interpenetrating arrays (Table 10)

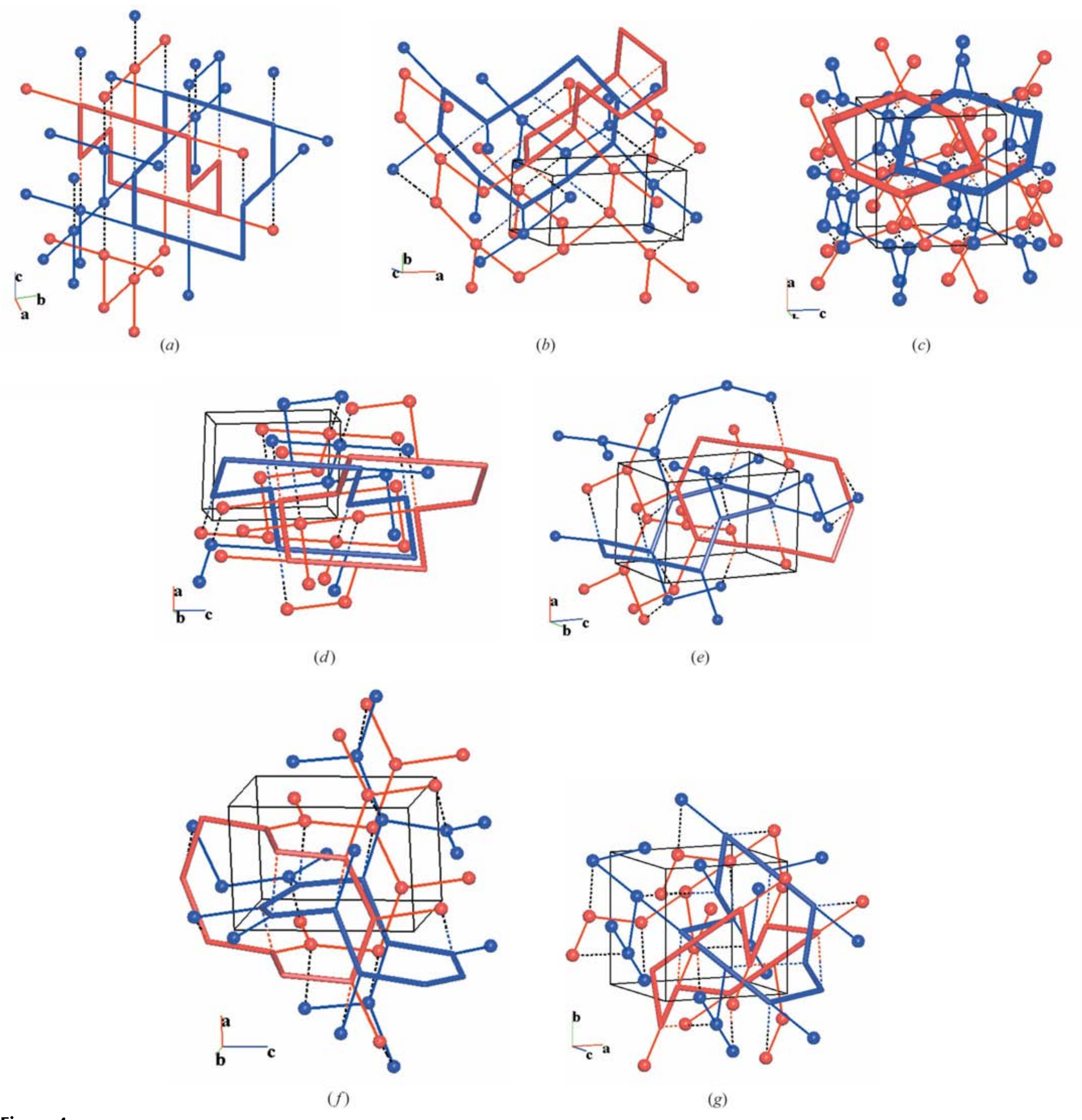

Figure 4
Relations between a set of two **ths** nets and the nets: (*a*) **cds**; (*b*) **dmp**; (*c*) *sqc*2075; (*d*) **tcb**; (*e*) **unm**; (*f*) **upa**; (*g*) 4/5/*t*2. Different **ths** nets are differently coloured. The edges to be broken in the initial nets are dotted. In each case, a couple of catenating 10-rings of the **ths** nets is selected. In *sqc*2075, some edges of intersecting 10-rings cross each other.

have large NRG degrees, *i.e.* they could be intermediate structures in many phase transitions.

Thus, large NRG degree is an important topological criterion for the net to be of interest in crystal chemistry. The following physical model may be proposed to support such an approach. Let us consider a liquid near the crystallization point when most of the atoms are close to the positions in the subsequent crystal. At this moment, not all interatomic bonds are formed: the liquid 'searches' for an appropriate topology by breaking existing contacts and forming new ones. In other words, the liquid passes over many topologies that are associated by supernet–subnet relations. Certainly, at this stage, the nets are not periodic, but they may be considered to be isomorphic to three-periodic nets. As a first approximation, one may expect that the system will most often pass over the nets that have many relations with super/subnets, *i.e.* have a large NRG degree. Therefore, with a high probability, the system will have the topology of one of these nets after crystallization. If one assumes that Nature prefers high-symmetry (uninodal and/or edge-transitive) nets (Ockwig *et al.*, 2005), then the nets listed in Tables 8–10 should draw attention as the most suitable templates for crystal engineering.

Obviously, the NRG degree is not the only criterion for the crystallochemical 'significance' of a net. As was mentioned in §2.2, a short adjacency sequence indicates that the net is near the 'centre' of the NRG, *i.e.* easily attainable from other nets.

Table 10
The interpenetrating net arrays with largest NRG degrees depending on the net coordination.

Node degree	Net	*Z*	NRG degree	MOFs†	Inorganic†
3	**dia-f** (3/4/*t*1)	4	839		
	ths (3/10/*t*4)	2	814	2	2
	srs (3/10/*c*1)	2	785	1	1
	utp (3/10/*o*1)	2	667		
	srs (3/10/*c*1)	4	525	‡	
	dia-f (3/4/*t*1)	2	259	‡	
	lig (3/8/*t*1)	4	252		
	lig (3/8/*t*1)	2	221	‡	
	ths (3/10/*t*4)	3	191	‡	
	dia-f (3/4/*t*1)	3	153		
4	**dia** (4/6/*c*1)	2	826	1	1
	sra (4/4/*o*1)	2	779	3	‡
	irl (4/4/*o*2)	2	557	‡	
	lvt (4/4/*t*1)	2	404	‡	‡
	uoc (4/4/*t*2)	2	313		
	dia-a (4/3/*c*6)	4	278		
	4/4/*t*37	2	271		
	crb (4/4/*t*5)	2	201		
	5/4/*t*5-4-*Pnnn*	2	183		
	5/4/*t*5-4-*C*222	2	168		

† Position in the list of occurrence of interpenetrating uninodal nets of a given coordination in metal-organic (Blatov *et al.*, 2004) or inorganic (Baburin *et al.*, 2005) frameworks. ‡ The number of cases is three or less.

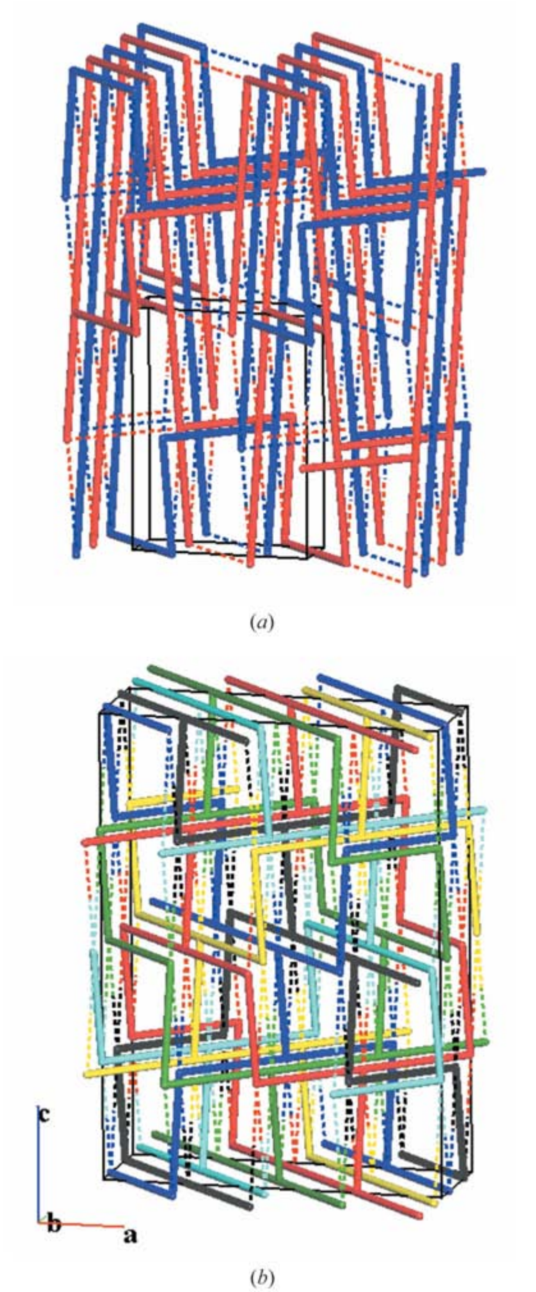

Figure 5
Relations between two- and sixfold **ths** arrays and a **roa** net. Breaking dotted edges in the initial **roa** net results in (*a*) a twofold and (*b*) a sixfold **ths** array. Different nets in the arrays are differently coloured.

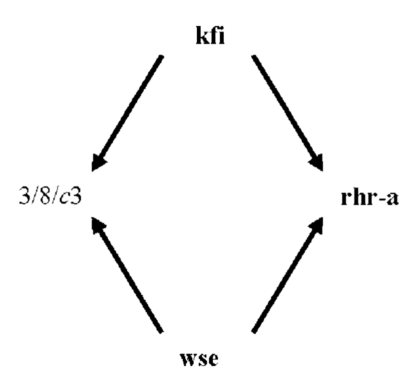

Figure 6
A part of the NRG consisting of four nets. The arrows indicate decrease of node degree during the corresponding supernet–subnet transition.

However, the length of the adjacency sequence is found to be non-characteristic: all the nets with a large NRG degree have adjacency sequences of length 8–10; the shortest length (8) occurs for the net **bnn**. It seems more important to consider other terms of adjacency sequence in addition to N_1. Thus, the value of N_2 is equal to the number of nets that can be transformed to a given one in two steps. Since the mechanisms of phase transitions do not assume a larger number of steps, as a rule, the nets with large N_1 and N_2 are of special interest. They are indicated at the top of Fig. 7; many of them are at the head of the lists in Tables 9 and 10. Moreover, according to Fig. 7, there are three distinct groups of nets in the NRG: (i) the nets with extremely large N_1; they are collected in Table 8 and scattered in the right part of Fig. 7; (ii) the nets with large N_2 (>2000); many of them also have a large N_1 (top left part of Fig. 7); (iii) the nets with N_1 not large and $N_2 < 2000$ (bottom left part of Fig. 7). Obviously, the last group contains crystallochemically 'insignificant' nets.

4. Concluding remarks

The results presented above demonstrate that one of the most important problems of modern crystal chemistry, the determination of suitable topological motifs for systems of interatomic bonds in crystals, may be considered from a new viewpoint. The proposed criteria for crystallochemically 'significant' nets are based on supernet–subnet relations and, being purely topological, are independent of geometrical properties of crystal structures, such as unit-cell dimensions or features of atomic packings. They rest upon the criteria introduced by Ockwig *et al.* (2005), but extend their list and turn from general symmetry properties of nets to a more detailed consideration of their topological peculiarities. Obviously, the topological criteria should be used along with well known crystallochemical descriptors referred to local (stereochemical) or global (packing) geometrical properties of crystals. Certainly, the uninodal nets do not cover all crystallochemically 'significant' topological motifs. At least two other groups of nets, edge-transitive and binodal, should be studied to make the analysis more complete. They will be treated in a further publication.

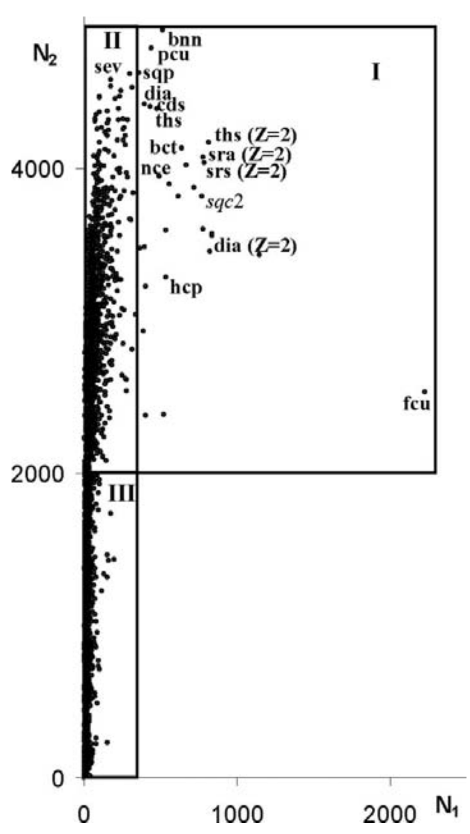

Figure 7
The distribution of the uninodal nets depending on the first two terms, N_1 and N_2, of their adjacency sequences in the NRG. The three groups of nets are separated by rectangles. Some important nets are designated.

APPENDIX *A*
Basic definitions

A ***net*** is a kind of graph that is *simple* (without loops and multiple edges; the edges are undirected) and *connected*, *i.e.* each graph vertex is accessible from any other vertex through a chain of edges; the vertices of the graph are called *nodes* of the net. A certain set of net edges (or pairs of adjacent nodes) determines net *topology*. Two nets are *isomorphic* if there are one-to-one correspondences between their sets of nodes and edges. The net is *periodic* if its symmetry group contains a subgroup of translations. The net is *uninodal* and *edge-transitive* if all its nodes and edges are symmetrically equivalent. A net is *n-coordinated* if the degree of any of its nodes is equal to *n*.

A ***subnet*** (***supernet***) of a net *A* is a net whose sets of nodes and edges are subsets (supersets) of corresponding sets of *A*.

A ***labelled quotient graph*** is a finite graph whose vertices and edges correspond to sets of translationally equivalent net nodes and edges. It may have multiple edges and loops if corresponding net edges connect translationally different or translationally equivalent nodes, respectively.

An ***embedding*** of a net is its realization in a space. *Euclidean* embeddings are of special interest for crystal nets. In this paper, we mainly consider *faithful* Euclidean embeddings where net nodes do not coincide with each other and there are no crossings between edges.

A ***three-dimensional net*** is a net that has an embedding into a three-dimensional space.

A ***coordination sequence*** $\{N_k\}$ is a set of sequential numbers $N_1, N_2, \ldots$ of nodes in first, second *etc*. coordination shells of a node in the net. The node *degree* is equal to N_1, and the node is called *N_1-coordinated*.

A ***circuit*** (*cycle*) is a closed chain of connected nodes.

A ***ring*** is a circuit without *shortcuts*, *i.e.* chains between two circuit nodes that are shorter than any chain between these nodes that belongs to the circuit.

An ***extended Schläfli symbol*** (*circuit symbol*) contains a detailed description of all shortest circuits for each angle (a couple of edges) at each inequivalent node.

A ***vertex symbol*** gives information similar to the extended Schläfli symbol, but for rings.

A ***net relation graph*** (NRG) is a graph whose vertices and edges correspond to nets and supernet–subnet relations between them.

The author thanks Professor M. O'Keeffe, Professor D. M. Proserpio, Dr S. T. Hyde, I. A. Baburin and an anonymous referee for many useful comments concerning the manuscript.

References

Baburin, I. A., Blatov, V. A., Carlucci, L., Ciani, G. & Proserpio, D. M. (2005). *J. Solid State Chem.* **178**, 2452–2474.
Blatov, V. A. (2006*a*). *Acta Cryst.* A**62**, 356–364.
Blatov, V. A. (2006*b*). *IUCr CompComm Newsletter*, **7**, 4–38.
Blatov, V. A., Carlucci, L., Ciani, G. & Proserpio, D. M. (2004). *CrystEngComm*, **6**, 377–395.
Carlucci, L. Ciani, G. & Proserpio, D. M. (2007). *Making Crystals by Design. Methods, Techniques and Applications*, edited by D. Braga & F. Grepioni, pp. 58–85. Darmstadt: Wiley.
Delgado-Friedrichs, O., Foster, M. D., O'Keeffe, M., Proserpio, D. M., Treacy, M. M. J. & Yaghi, O. M. (2005). *J. Solid State Chem.* **178**, 2533–2554.
Delgado-Friedrichs, O. & O'Keeffe, M. (2003). *Acta Cryst.* A**59**, 351–360.
Delgado-Friedrichs, O. & O'Keeffe, M. (2005). *J. Solid State Chem.* **178**, 2480–2485.
Delgado-Friedrichs, O., O'Keeffe, M. & Yaghi, O. M. (2006). *Acta Cryst.* A**62**, 350–355.
Eon, J.-G. (2005). *Acta Cryst.* A**61**, 501–511.
Hyde, S. T., Delgado-Friedrichs, O., Ramsden, S. J. & Robins, V. (2006). *Solid State Sci.* **8**, 740–752.
International Tables for Crystallography (2004). Vol. A1, edited by H. Wondrachek & U. Müller. Dordrecht/Boston/London: Kluwer Academic Publishers.
Klee, W. E. (2004). *Cryst. Res. Technol.* **39**, 959–968.
Klein, H.-J. (1996). *Math. Model. Sci. Comput.* **6**, 325–330.
Koch, E. & Fischer, W. (1995). *Z. Kristallogr.* **210**, 407–414.
Koch, E., Fischer, W. & Sowa, H. (2006). *Acta Cryst.* A**62**, 152–167.
Leoni, S. & Zahn, D. (2004). *Z. Kristallogr.* **219**, 339–344.
Ockwig, N. W., Delgado-Friedrichs, O., O'Keeffe, M. & Yaghi, O. M. (2005). *Acc. Chem. Res.* **38**, 176–182.
Öhrström, L. & Larsson, K. (2005). *Molecule-Based Materials. The Structural Network Approach.* Amsterdam/Oxford/San Diego/London: Elsevier.
O'Keeffe, M. (2006). Private communication.
O'Keeffe, M. & Hyde, B. G. (1996). *Crystal Structures. I. Patterns and Symmetry*. Washington, DC: Mineralogical Society of America.
Peresypkina, E. V. & Blatov, V. A. (2000). *Acta Cryst.* B**56**, 1035–1045.
Sowa, H. (2005). *Acta Cryst.* A**61**, 325–330.
Sowa, H. & Koch, E. (2001). *Acta Cryst.* A**57**, 406–413.
Sowa, H. & Koch, E. (2002). *Acta Cryst.* A**58**, 327–333.
Wells, A. F. (1954). *Acta Cryst.* **7**, 535–544.
Wells, A. F. (1977). *Three-Dimensional Nets and Polyhedra.* New York: Interscience.